Global Journal of Biotechnology & Biochemistry 7 (4): 100-109, 2012
ISSN 2078-466X

DOI: 10.5829/idosi.gjbb.2012.7.4.1105

Design of Multifunctional H3 Receptor Inverse Agonists with Ache Inhibitor Activity for Treatment of Alzeihmer's Disease

Akalabya Bissoyi, Divyanshu Mahajan and Biswadeep Chaudhuri

Department of Biotechnology and Medical Engineering,
National Institute of Technology Rourkela, Orissa, India

Abstract: Acetyl cholinesterase (AchE) and *N*-methyl-D-aspartate antagonists are at present the only commercially available treatment for Alzheimer's disease (AD). Histamine H3 receptor antagonists are used for the treatment of several neurodegenerative disorders such as Epilepsy, Alzheimer's and Parkinson's diseases. Both H3 and AchE inhibitors alleviate the symptoms of Alzheimer's disease by enhancing the acetylcholine levels in the brain but the mechanism of action involved in both the cases is different. Here, it is proposed that histamine H3 antagonist with AchE inhibitor activity can be used as a novel class of drugs to treat Alzheimer's disease with lesser adverse peripheral effects than excessive AchE inhibitor alone. Thus the main objective of this work is to design multifunctional inhibitors for reduction of the side effects of the already available drugs. This study is divided into two parts. In the first part, homology modeled structure of histamine H3 active site and available crystal structure of AchE was used to collect the information for identification of pharmacophore. The important descriptors were identified based on comparative 2D-QSAR and 3D-QSAR study of 28 drug-like compounds for histamine H3 receptors collected from the literature. In the second part, five hybrid molecules were generated based on the pharmacophore of histamine H3 receptor and known pharmacophore of AchE inhibitors. All five hybrid molecules were screened through ADME/Tox filters. The hybrid molecule was validated through GOLD docking score in both AchE and histamine H3 receptors. The best hybrid compound was then evaluated by molecular dynamics (MD) simulation in water solvent model using 3D model of human histamine H3 receptor (build based on bovine rhodopsin structure).

Key words: Alzheimer's disease · Histamine H3 receptors · AchE inhibitors · Docking · QSAR · GROMACS

INTRODUCTION

The neurodegenerative dementias are progressive and irreversible due to deterioration of brain cells and their interconnections. Alzheimer's disease (AD) is the most common form of progressive and irreversible neurodegenerative dementia [1]. It is characterized by cognitive deterioration of neurons and synapses in the cerebral cortex and certain subcortical regions [2]. AD affects the memory, thinking and behavioral skills as well as causes problems with language, decision-making ability, judgment and personality. It is caused due to genetic or environmental factors but the exact cause is still unknown. The goal in treating AD is to decrease the progression of the disease and manage the behavior problems, confusion, sleeplessness and agitation. Therapeutic treatment is aimed at slowing the rate at which symptoms become worse as AD can't be cured [3]. The most frequently prescribed anti-Alzheimer's drugs are the acetylcholinesterase (AchE) inhibitors, which promote memory function and delay the cognitive decline without altering the underlying pathology [4]. However, their efficacy is limited and they are associated with unpleasant side effects.

Histamine receptors are G-protein coupled receptor and can be broadly classified into 4 subtypes as H1, H2, H3 and H4 [5]. H3 receptors are widely expressed in the mammalian brain especially in the areas involved in cognitive processes and arousal such as the cerebral cortex, hippocampus, basal ganglia and hypothalamus [6]. Selective antagonists of histamine H3 receptors can increase the release of neurotransmitters like Acetylcholineestrase (AchE) involved in cognitive processes in vivo and may have implications for the

Corresponding Author: Akalabya Bissoyi, Department of Biotechnology & Medical Engineering,
National Institute of Technology Rourkela, Orissa, India.

treatment of degenerative disorders associated with impaired cholinergic function [6, 7]. AchE inhibitors increase the synaptic levels of acetylcholine by preventing release of AchE into the synaptic cleft, thus promoting cholinergic neurotransmission whereas histamine H3 receptor antagonists via a discrete mechanism increase the neurotransmitter release from the synaptic vesicle [8]. Histamine H3 receptor antagonists increase cholinergic neurotransmission and AchE inhibitors enhance the half life of AchE in the synapse thus increasing the probability of interaction with receptors on postsynaptic cell to elicit a biological response [9]. A molecule that combines the properties of AchE inhibitor and histamine H3 receptor antagonist would enhance the levels of chemical signaling than either an AchE inhibitor or a histamine H3 receptor antagonist alone. A combination molecule will require lower dosage and have a higher potency for increasing acetylcholine levels thus improving the side effect profile.

This study describes the molecular modeling efforts that lead to the identification of an AchE inhibitor-histamine H3 receptor antagonist. The use of available crystal structure information of AchE receptor, homology model structure of H3 receptor based on bacterial rhodopsin crystal structure, pharmacophore modeling, QSAR, rigid docking and molecular dynamic simulation lead to this discovery.

MATERIALS AND METHODS

Methodology: Sequence alignment and homology modeling: The transmembrane portion of the histamine H3 receptor was built by homology modeling techniques using 2.8 angstrom resolution crystal structure of Bovine Rhodopsin (PDB 1HZX) as template structure [13]. The primary sequence of the histamine H3 receptor was aligned with Bovine Rhodopsin based upon highly conserved amino acid residues in the seven helices, using the CLUSTALW program (http://www2.ebi.ac. uk/ CLUSTALW) [14]. The initial sequence-structure alignment was based on multiple sequence alignments. All homology models were constructed with the SWISS-MODEL server (http://expasy.org/swissmod) [9-11] and amino acid side chain conformations were added using program SCWRL3.0. [12]. The stereo chemical qualities of the model were checked with (http://nihserver.mbi.ucla.edu/SAVS/). Finally, the structural properties of the target protein were validated by using the Ramachandran plot score.

Molecular Redocking Studies H3 and Ache Receptors with Known Active Molecules

Preparation of Ligands and Protein: Since ligands are not peptides, Gasteiger charges were assigned to the ligands and then non-polar hydrogen atoms were merged. Tacrin was used as histamine H3 receptor inhibitor and Rivastigmine was used as AchE inhibitor for docking studies. The rigid roots were defined automatically for each compound and the amide bonds were made non-rotatable. The homology model structure was used for docking study and Kollman charges were added to each atom of the modeled protein.

Grid Generation for H3 Receptor: The Grid box was centered on the Asp 114 of the human histamine H3 receptor. The binding site includes the catalytic center (Asp 114 and Glu 206) and several subsites as (Ser-79, Lec-82, Val-83, Gly-84, Phe-86, Cys-87, Ile-88, Pro-89, Leu-90, Tyr-91, Trp-100, Leu-106, Cys-107, Lys-108, Leu-109, Val-112, Val-113, Asp-114, Tyr-115, Leu-116, Leu-117, Cys-118, Thr-119, Ser-120, Trp-60, Trp160, Tyr-167, Gly-168, Ile-171, Glu-175, Phe-192, Phe-198, Glu-206, Trp-371, Tyr-374, Met-378, Tyr-394, Phe-398, Leu-401, Ser-405). The spacing between the Grid points was 0.375 angstroms.

Grid Generation for AchE Inhibitor: The Grid box was centered on the Ser 199, His 439 and Glu 326 of the AchE. The binding site includes several sub sites as (Tyr70, Trp84, Gly118, Tyr 121, Tyr130, Glu199, Ser200, Trp279, Leu282, Ile287, Phe288, Phe290, Glu327, Phe331, Tyr334 and His440). The spacing between the Grid points was 0.375 angstroms.

Qsar Study of Histamine H3 Receptor

Dataset: Dataset of 28 non-peptide inhibitor molecules described by [15], were considered in this study (Fig. 4). All the molecules studied had the same parent skeleton.

2D QSAR Study

Generation of Molecular Descriptors: PRODRG software was used to build and perform energy minimization on the 28 selected inhibitors and the output files were saved in mol2 format [16]. The inhibitors were divided into Test set and Training set in 1:4 ratio such that the Test set had maximum and minimum IC_{50} value that falls within the IC_{50} values of Training set. The output files were loaded into 'VlifeMDS QSAR' module (VLifeMDS: Molecular Design Suite, 2010) for evaluation of several molecular descriptors and to build a QSAR equation, which can further be used

to predict the activity of test/new molecules (www.vlifesciences.com). This module can calculate all the physiochemical descriptors such as Individual, Chi, Chiv, Path count, Chi Chain, Chiv chain, chain path count, Cluster, Path cluster, Kappa, Element count, Estate numbers, Estate contributions, Information theory index. Deselect Dipole Moment, Electro Static, Distance Based Topological Indices, Semi Empirical and Hydrophobicity base logP descriptors (as these are 3D descriptors).

3D QSAR Study

k-Nearest Neighbor QSAR: In k-nearest neighbor algorithm for classifying a new pattern (molecule), the system finds the 'k' number of nearest neighbors among the training set and uses the different categories of the k-nearest neighbors to weight the category candidates [17]. The nearness is measured by an appropriate distance metric (e.g. a molecular similarity measure, calculated using descriptors of molecular structures).

Molecular Synamic Simulation Study: MD simulations were performed using the GROMACS molecular dynamics program [18] version 3.3.1 with the OPLS-AA force field [19-20]. Berendsen thermostat was used for maintaining the temperature. The pressure was maintained to a reference pressure of 1 bar with a coupling time of 1 ps. Interactions within the larger cut-off were updated every 10 steps. The time step used was 2 fs. The simulations lasted for 1 ns and were carried out at temperature of 310°K. The potential energy and root mean square distance (RMSD) values were plotted versus the simulation time to judge whether the simulations had reached a level of equilibrium.

RESULTS AND DISCUSSION

Sequence Alignments and Modeling H3 Receptor: Sequence alignment was done with the help of CLUSTALW software using default parameters. Because of an overall 60% sequence identity between the template and the target (Fig. 1), the generation of homology model of the human histamine H3 receptor was done using online Swiss model server (www.expasy.ch/swissmod/SWISS-MODEL.html) based on the backbone coordinates of the crystal structure 1HZX of bovine Rhodopsin [21]. he missing side chain was added using the program SCWRL3.

PROCHEK was used to check the stereo chemical quality of the protein structure generated, by analyzing residue-by-residue geometry and overall structural geometry [22]. It provides information about covalent geometry, Planarity, Dihedral angles, Chirality and Non-bonded interactions. The Ramchandran plot of the protein model (Fig. 2) was generated by PROCHEK.

Redocking Study: All the 28 molecules were docked with the homology modeled structure of histamine H3 receptor using Autodock4 software [23]. The docking results were ranked according to the decreasing docking energies of the 100 conformers for each of the molecules. It was found that molecules with lowest docking energies interacted quite well with the receptor in the pocket. The molecules 11, 18, 23, 25 and 26 had scores less than -8.00 kcal/mol (Table 1). The AchE receptor's PDB structure 1EVE and 1GQR were considered for docking studies with Rivastigmine as ligand molecule [24-25]. Rivastigmine interacted better with the receptor binding pocket of PDB structure 1EVE (Fig. 3) with a docking score $\leq$ -11.30 kcal/mol (Table 2) and hence 1EVE was used for further investigations.

Residue Interacting with the Ache Receptor: The 28 molecules used divided into two parts; one is Test set and other being Training set. Different 2D QSAR methods were used such as SW, GA, MR using the Training set and Test set. 2D QSAR showed different q^2 values which ranged from 0.4986 and 0.8222, with different q^2 values for different descriptors. To make a common set out of the entire 20 different descriptors, a QSAR model was built using the neural network. The q^2 value thus generated was more than 0.89 (i.e. around 90% in prediction of IC50 value).

QSAR Model Using Neural Network: Back propagation Training set size=23, Test set size=5 selected descriptors-ChiV1, Polar surface area excluding PandS, SaaCHcount, T_T_N_4, T_2_2_6, T_2_2_5, T_O_O_2, SssOcount, T_2_C_4, T_2_2_5,T_C_N_7, SssOHcount, T_C_F_3, SsCH3E-index, T_C_N_6, T_2_2_5, SssOE-index, T_O_O_7,T_O_O_2,T_O_O_0,, T_2_2_0, T_T_N_3,CHIv0,T_2_2_4, SsOHE-index. Statics- N=23, degree of freedom=1, r2 =0.9595, F Test =1.1278, pred_r2 =0.7382, pred_r2se =0.3132.

Interpretation and Comparison of SW-KNNMFA and SA-KNNMFA 3D QSAR Model: Two variable selection methods have been used to obtain the KNNMFA models. The study shows that steric potential (1 out 3 in SW and 3 out of 3 in SA) and the descriptors S_275 are common in both generated models. Descriptors range for

Table 1: Binding free energies for the 28 molecules after docking with histamine H3 receptor.

Sl.No.	Compounds	Estimated Free Energy of Binding (kcal/mole)	Estimated inhibition (μm)	Final intermolecular energy (Vdr +H-bond +Dissolved energy) in kcal/mole	Final total internal energy (kcal/mole)	Torsional free energy (kcal/mole)	Unbound system energy (kcal/mole)
1	Compound 1	-7.84	1.75	-8.45	+0.12	+1.10	-0.62
2	Compound 2	-7.71	2.23	-8.62	-0.61	+1.10	-0.42
3	Compound 3	-7.31	4.41	-8.16	-0.65	+1.10	-0.41
4	Compound 4	-6.37	3.83	-8.22	-0.67	+1.10	-0.41
5	Compound 5	-7.85	1.75	-8.68	-0.69	+1.10	-0.42
6	Compound 6	-7.08	6.48	-7.96	-0.68	+1.10	-0.44
7	Compound 7	-6.20	28.59	-6.91	0.73	+1.10	-0.35
8	Compound 8	-7.18	5.41	-8.94	-0.59	+1.92	-0.43
9	Compound 9	-5.64	72.90	-7.10	-0.89	+1.92	-0.43
10	Compound 10	-6.88	9.03	-8.09	-0.80	+1.37	-0.64
11	Compound 11	-8.15	1.07	-9.04	-0.64	+1.10	-0.44
12	Compound 12	-6.17	30.26	-7.15	-0.50	+1.10	-0.38
13	Compound 13	-6.14	31.36	-7.95	-0.85	+2.20	-0.46
14	Compound 14	-7.14	5.86	-9.17	0.64	+2.20	-047
15	Compound 15	-7.57	2.81	-8.68	-0.72	+1.37	-0.46
16	Compound 16	-7.14	3.71	-8.82	-0.43	+1.37	-0.47
17	Compound 17	-7.57	2.84	-8.85	-0.63	+1.37	-0.54
18	Compound 18	-8.54	0.547	-9.45	-0.61	+1.65	-0.43
19	Compound 19	-7.85	1.70	-8.48	-0.12	+165	-0.43
20	Compound 20	-6.88	8.99	-7.91	-0.53	+1.10	-0.45
21	Compound 21	-7.06	6.68	-7.87	-0.74	+1.10	-0.45
22	Compound 22	-7.60	2.07	-8.97	-0.80	+1.65	-0.53
23	Compound 23	-8.43	0.66	-9.60	-0.72	+1.37	-0.52
24	Compound 24	-7.45	3.46	-8.96	-0.57	+1.65	-0.43
25	Compound 25	-8.01	1.34	-9.48	--0.61	+1.65	-0.43
26	Compound 26	-8.00	1.37	-8.88	-0.65	+1.10	-0.43
27	Compound 27	-7.27	4.71	-8.28	-0.44	+1.10	-0.36
28	Compound 28	-6.44	19.01	-7.08	-0.84	+1.10	-0.38

Table 2: Binding free energies for the pharmaceutical compound Rivastigmine with PDB structures (1EVE, 1GQR).

Sl.no	Compounds	Estimated Free Energy of Binding (kcal/mole)	Estimated inhibition (μm)	Final intermolecular energy (Vdr +H-bond + Dissolved energy) in kcal/mole	Final total internal energy (kcal/mole)	Torsional free energy (kcal/mole)	Unbound system energy (kcal/mole)
1	1EVE-RIVASTGMINE	-11.35	4.75nm	-12.98	-0.70	+1.65	-0.68
2	1GQR-RIVASTGMINE	-9.63	86.82nm	-10.18	-0.20	-1.37	-0.01

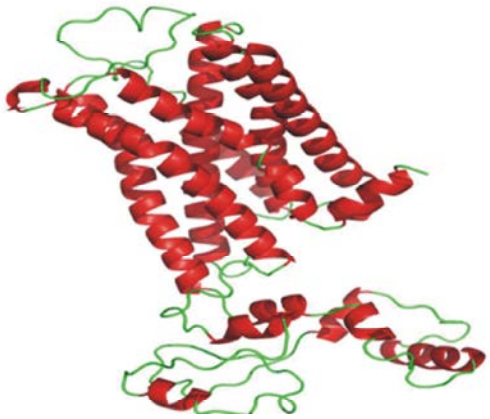

Fig. 1: Structure Analysis and Verification.

SA-KNNMFA are Electrorostatic -E_ 655(30.0000, 30.0000), E_584 (10.0000, 10.00000) Steric potential -S_725 (7.7104, 30.0000). Descriptors range for SW-KNNMFA are Steric potential -S_725 (7.7104, 30.0000), S_795 (-0.3099, 30.0000) and S_675 (-0.0113, 30.0000). Positive range indicates that positive electrostatic potential is favorable for increase in the activity and hence a less electronegative substituent group is preferred in that region. Negative range indicates that negative steric potential is favorable for increase in the activity and hence less bulky substituent group is preferred in that region. Positive range indicates that positive steric potential is favorable for increase in the activity and hence more bulky substituent group is preferred in that region.

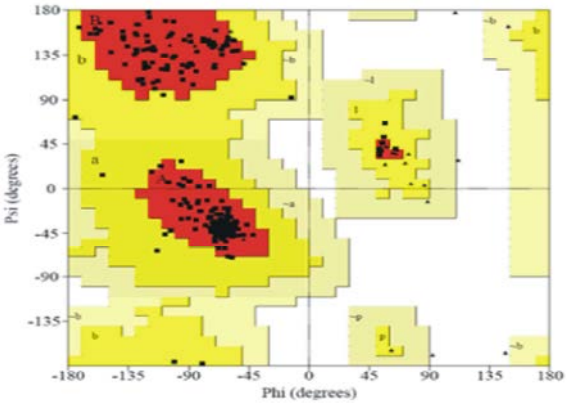

Plot statistics Residues in most favored regions [A,B,L]	306	
90.3%		
Residues in additional allowed regions [a,b,l,p]	24	
7.1%		
Residues in generously allowed regions [~a,~b,~l,~p]	6	
1.8%		
Residues in disallowed regions	3	
0.9%		
Number of non-glycine and non-proline residues	339	
100.0%		
Number of end-residues (excl. Gly and Pro)	2	
Number of glycine residues (shown as triangles)	32	
Number of proline residues	23	
Total number of residues	396	

Residue in disallow region are HIS417. THR-149. SER-330

Fig. 2: Ramchandran plot of human histamine H3 receptor protein from PROCHECK. The three disallowed residues are not part of the active site of the receptor and thus the derived model is stable.

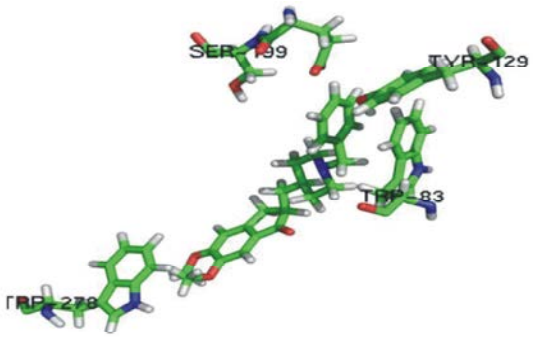

Fig. 3: Rivastigmine within the binding pocket of 1 EVE.

Pharmacophore Study of AchE Inhibitor: After redocking study using crystal structure of Rivastigmine in the active site of AchE, two sets of key interactions between the protein and the ligand were deduced. One set of interaction between the Trp83 (located at the base of the active site) and quaternary amine of Rivastigmine and second interaction of Trp278 located at the opening of the cavity.

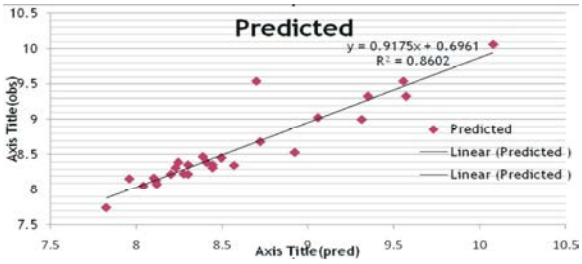

Fig. 4: Plot of the observed vs. calculated pki values of the binding affinities to the H3 receptors.

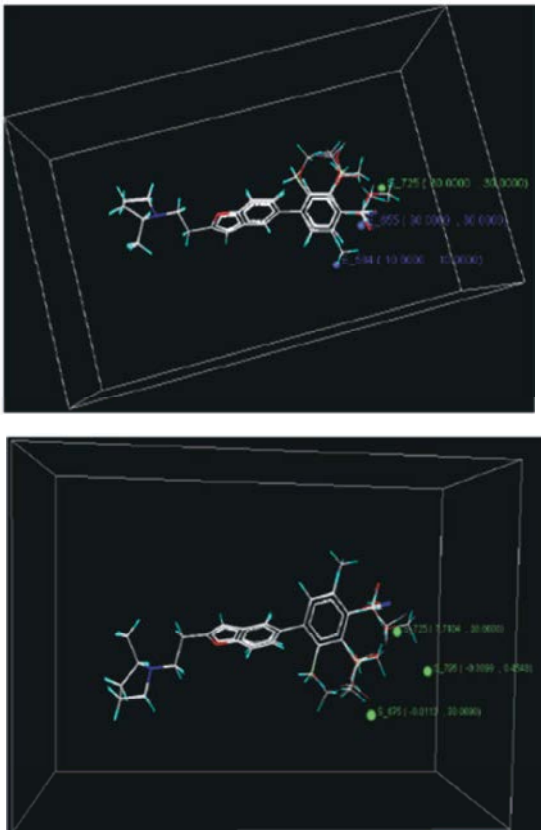

Fig. 5: Comparison of two variable selection models used for QSAR study. Distribution of chosen points a) in the SA kNN-MFA for the aryl benzo data set with the selected test set molecule. b) in the Sw kNN-MFA for the aryl benzo data set with the selected test set molecule.

Molecular Hybrid: Hybrids can be designed as histamine H3 receptor antagonist capable of inhibiting AchE using the crystal structure data of AchE (1EVE) and knowledge obtained from 2D QSAR, 3D QSAR and 3D pharmacophore of histamine H3 receptor. Molecular hybridization of histamine H3 receptor antagonists and

(a)

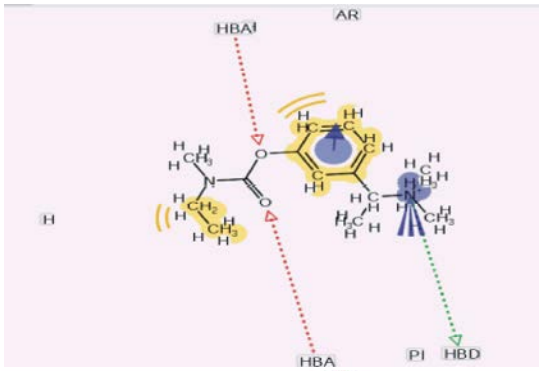

(b)

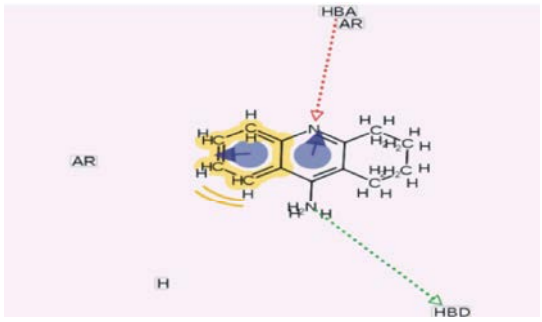

Fig. 6: Redocking study. a) Pharmacophore of Rivastigmine and b) Pharmacophore of Tacrine based on redocking study.

AchE inhibitors was carried out using their pharmacophores and it was found that quaternary amine of both structures fit well. A total of 5 hybrids with best IC_{50} value were designed using Rivastigmine for AchE inhibitor activity (Fig. 6a) and Tacrine for histamine H3 antagonist activity (Fig. 6b). The hybrid molecules (Fig. 7) were passed through Lipinski five rules and toxicity predictions were done through ADME/TOX filter [26-27].

Validation of Five Hybrids: Out of the five hybrids, the binding mode of hybrid 3, 2, 4 very much overlaid with the crystal structure binding mode of decamethonium 1EVE. Good superposition between the Donepezil structure oriented with GOLD and the same molecule in the crystallographic orientation suggest the appropriateness of the used method as shown in Fig. 8 [28-30]. The conformation of highest score obtained with GOLD for this proposal-3 (score=81) and it almost align with the Rivastigmine. Donepezil in PDB and for histamine H3 receptor proposed compound shows highest score.

Molecular Dynamic Simulation MD Simulation: The best ligand-receptor complex determined by docking calculation, were placed in a box of water using algorithms

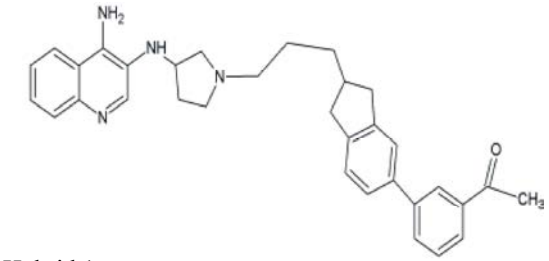

Hybrid 1

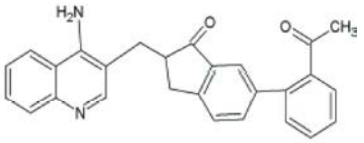

Hybrid 2

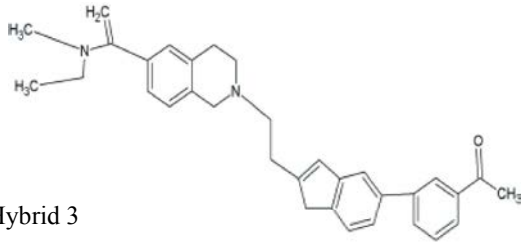

Hybrid 3

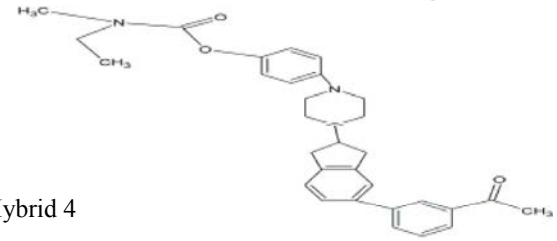

Hybrid 4

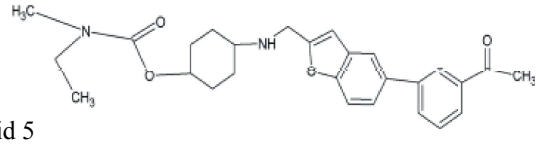

Hybrid 5

Fig. 7: Molecular hybrids with arylbenzofuran. Hybrid 1 and 2 were derived by molecular hybridization of Tacrine with arylbenzofuran. And Hybrids 3, 4, 5 were derived by molecular hybridization of Rivastigmine with arylbenzofuran.

and simulated for 1ns after initially equilibrating with water molecules for 50 ns. An average structure was energy minimized under conjugated gradient and periodic boundary condition. The dynamic behavior and structural change of the receptor was analyzed by calculating the RMSD value for structural movement and changes in the secondary structural elements of the receptor model during the MD simulation. The structural changes of histamine H3 receptor model were evaluated during 1ns MD simulation using GROMACS 3.3.1 [32-33].

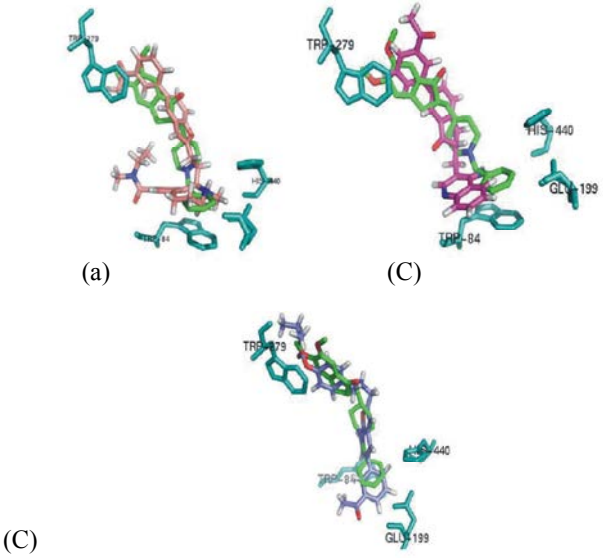

Fig. 8: Validation of the top ranked hybrids. Details of the AchE active site in which the superposition of the crystallographic orientation of donepezil with the top 3 ranked solution suggested by GOLD is shown. Donepezil is shown in green colour.

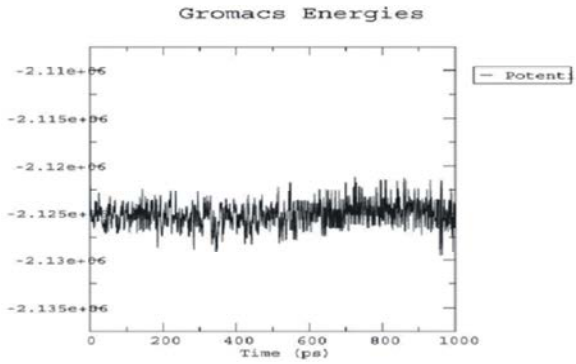

Fig. 9: Potential energy graph of protein-ligand complexes. The potential energy graph during 1ns molecular simulation in the active site showing stability of the complex formed using GROMACS 3.3.1.

It can be seen from Figure 9 that the potential energy of the histamine H3 receptor model Ligands reaches to the plateau (2.0 A) within the first 200 ps. Potential energy of protein-ligand complex remain in range between - 2.12e+06 to -2.13e+06 KJ/mol [34].

It can be clearly seen from the plots that the complex as well as the protein become stable after 460ps simulation and the histamine H3 receptor backbone reaches a constant level after 250 ps at 86 2.0 A°, but suddenly

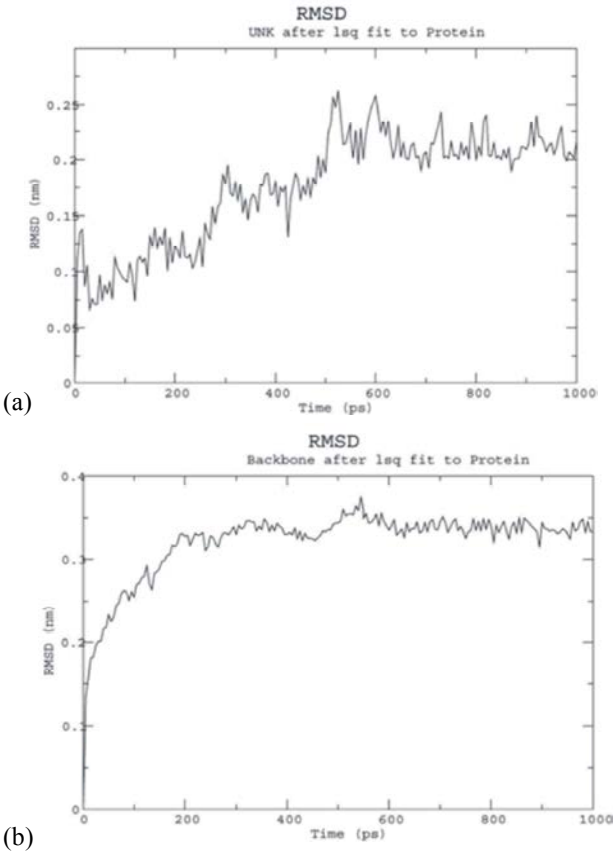

Fig. 10 a: Plot showing the RMSD deviation of ligand in the solvated protein during 1ns molecular simulation in the active site using GROMACS 3.3.1 b) RMSD graph showing solvated protein.

increases after 460 ps at 2.5 A° and then remain same for 1ns simulation time period. The H-bond between drug molecule and enzyme were analyzed and after calculating the average of all H-bond candidates total 3 H-bonds were observed between ligand and receptor molecule. The RMSD plots of protein backbone and the drug were obtained separately (Fig. 10 a) and b) respectively). The backbone RMSD indicates that the rigid protein structure equilibrates rather quickly in this simulation (after 20 ps). The drug does not equilibrate until after 30 ps. The RMSD for the drug is more variable indicative of its mobility within the binding pocket. The RMSD close to 3.5A0 (for backbone) and 2.5 A0 (for drug molecule) and fairly low potential energy close to -2.12e+06 to - 2.13e+06 KJ/mol shows high stability of protein-ligand complex shows the likeliness of ligand molecule to be drug like candidates.

CONCLUSION

In the above study, combined 2D QSAR study was carried out using various statistical models. Using all the models, 20 best descriptors were selected and used in neural network back propagation model as a training set to conclude to a given result (Table 3 and 4). The value of cross validated squared correlation coefficient -q^2 generated more than 0.89 (i.e. around 90% accurate in prediction of IC50 value) suggests a good internal productivity of the equation. The equation generated describes the positive contribution of Chiv 0, SssOE-index, SssCH3-index, Polar Surface Area excluding P and S whereas Chiv1, SssO count, SaaCHcount descriptors contributed negative to the inhibitory activity. From 3D QSAR study using SW kNN-MFA and SA kNN-MFA shows that steric potential (1 out of 3 descriptors in SA, 3 out of 3 descriptors in SW are steric potential descriptors) plays major role in determining biological activity. The descriptor S_725 (7.7104, 30.0000) was common in both g enerated model. Statistically, SW kNN-MFA model is comparatively better as compared to SA kNN-MFA with respect to q^2=0.6154. In the second part of this work, five novel molecular hybrids of the pharmaceuticals Tacrine, Rivastigmine and aryl benzofuran used in the treatment of Alzheimer‘s disease (AD) were designed and evaluated for further investigation and experimental validation. Based on this work, the hybrids proposed have shown very close orientations to the original pharmaceuticals. Our results suggest that the Proposal-3 with highest synthetic viability has more interactions with both AchE and histamine H3 receptor. During molecular dynamic studies done with H3 receptor using GROMACS, the amino acid residues responsible for the formation of the hydrogen bonding with TYR-59 (tyrosine residue number 59) were identified. We propose that this molecule is an interesting pharmaceutical candidate for preparation and further investigation in Laboratory.

Table 3: Comparison of the MR, SA-MR, GA-MR, PLS, SA-PLS, GA-PLS, PCR, SA-PCR, GA-PCR models for the aryl benzo data set using the selected data set.

Parameter/molecule		MR	SA-MR	GA-MR	PLS	SA-PLS	GA-PLS
r^2		0.7602	0.7637	0.5977	0.8222	0.4986	0.7148
q^2		0.4869	0.4224	0.2859	-0.2345	-0.2630	0.2570
F-Test		20.0721	10.9900	9.4098	29.2872	9.9458	25.0679
r^2 se		0.2933	0.2850	0.3517	0.2338	0.3827	0.2886
q^2 se		0.4290	0.4455	0.4686	0.6161	0.6074	0.4659
pred_r^2		0.3206	0.6649	0.7019	0.8041	0.4175	0.7465
pred_r^2 se		0.5046	0.4602	0.4340	0.3519	0.6067	0.4002
Selected Descriptors	Actual	Polar surface area excluding P and S, SssOE-index, T_2_C_4.	T_2_2_5, T_C_N_7, SssOHcount, T_C_F_3, SsCH3E-index	Polar surface area excluding PandS, T_C_N_6, T_O_O_0.	Polar surface area excluding PandS, T_2_2_5, SssOE-index, T_O_O_7, T_O_O_2.	ChiV5, Polar surface area excluding PandS, T_2_2_0.	T_T_N_3, CHIv0, T_2_2_4, SsOHE-index, SsCH3E-index.
Molecule-2	9.569	9.3298	9.0263	9.0230	9.1737	8.8160	9.1278
Molecule-4	8.658	8.2758	8.3146	8.3474	8.3263	8.1845	8.4352
Molecule-8	8.244	8.3478	8.3650	8.3474	8.3263	8.1427	8.2833
Molecule-14	7.959	8.2537	8.3273	8.2184	8.2390	8.5731	8.2339
Molecule-27	8.699	9.5460	9.0197	9.0230	9.1737	9.0109	8.9878

Table 4: Comparison of the PCR, SA-PCR, GA-PCR model for the aryl benzo data set using the selected data set

Parameter/molecule	PCR(Forward)	SA-PCR	GA-PCR
r2	0.7646	0.7017	0.3254
q2	0.3449	0.2556	-0.0750
F-Test	20.5721	10.5836	10.1298
r2 se	0.2690	0.3112	0.4332
q2 se	0.4488	0.4916	0.5469
pred_r2	0.8450	0.6729	0.0858
pred_r2 se	0.3130	0.4546	0.7601

Selected Descriptors	Actual	Polar surface area excluding P and S, SssOE-index, T_2_C_4.	T_2_2_5, T_C_N_7, SssOHcount, T_C_F_3, SsCH3E-index	Polar surface area excluding PandS, T_C_N_6, T_O_O_0.
Molecule-2	9.569	9.3298	9.0263	9.0230
Molecule-4	8.658	8.2758	8.3146	8.3474
Molecule-8	8.244	8.3478	8.3650	8.3474
Molecule-14	7.959	8.2537	8.3273	8.2184
Molecule-27	8.699	9.5460	9.0197	9.0230

REFERENCES

1. Arnold, K., L. Bordoli, J. Kopp and T. Schwede, 2006. The SWISS-MODEL Workspace: A web-based environment for protein structure homology modelling. Bioinformatics, 22: 195-201.
2. Chomczynski, P. and N. Sacchi, 2007. MHP-133, a drug with Multiple CNS Targets: Potential for Neuroprotection and Enhanced cognition. Neurochem. Res., 32: 1224-1237.
3. **Missing**
4. Dorronsoro, I., A. Castro and A. Martínez, 2003. Peripheral and dual-binding site acetylcholinesterase inhibitors as neurodegenerative disease modifying agents. Exp. Opin. Ther. Pat., 13: 1725-1732.
5. Suh, W.H., K.S. Suslick and Y.H. Suh, 2005. Therapeutic agents for Alzheimer's disease. Curr. Med. Chem., 5: 259-269.
6. Dastmalchi, S. and M. Hamzeh-Mivehroud, 2008. Molecular modeling of histamine H3 receptor and QSAR studies on arylbenzofuran derived H3 antagonists. Journal of Molecular Graphics and Modelling, 26(5): 834-844.
7. Cowart, M., J.K. Pratt, A. Stewart, Y.L. Bennani, T. Esbenshade and A. Hancock, 2004. A new class of potent non-imidazole H3 antagonists: 2-aminoethylbenzofuranes. Bioorg. Med. Chem. Lett., 14: 689-693.
8. Massoulié, J. and S. Bon, 1982. The molecular forms of cholinesterase and acetyl cholinesterase in vertebrates. Annu. Rev. Neurosci., 5: 57-106.
9. Guex, N. and M.C. Peitsch, 1997. SWISS-MODEL and the Swiss-PdbViewer: An environment for comparative protein modelling. Electrophoresis, 18: 2714-2723.
10. Peitsch, M.C., 1995. Protein modeling by E-mail Bio/Technology, 13: 658-660.
11. Schwede, T., J. Kopp, N. Guex and M.C. Peitsch, 2003. SWISS-MODEL: an automated protein homology-modeling server. Nucleic Acids Research, 31: 3381-3385.
12. Canutescu, A.A., A.A. Shelenkov and R.L. Dunbrack Jr., 2003. A graph-theory algorithm for rapid protein side-chain prediction. Protein Science, 12: 2001-2014.
13. Palczewski, K., T. Kumasaka, T. Hori, C.A. Behnke, H. Motoshima, B.A. Fox, I. Le Trong, D.C. Teller, T. Okada and R.E. Stenkamp, 2000. Crystal structure of rhodopsin: A G protein-coupled receptor. Science, 289(5480): 739-45.
15. Gfesser, G., R. Faghih, Y. Bennani and M. Curtis, 2005. Stucture-Activity relationships of arylbenzofuran H3 receptor antagonists. Bioorg. Med. Chem. Lett., 15: 2559-2563.
16. Van Aalten, D.M., R. Bywater, J.B. Findlay, M. Hendlich, R.W. Hooft and G. Vriend, 1996. PRODRG, a program for generating molecular topologies and unique molecular descriptors from coordinates of small molecules. Journal of Computer-Aided Molecular Design, 10(3): 255-262.
18. Lindahl, E., B. Hess and D.V.D. Spoel, 2001. GROMACS 3.0: a package for molecular simulation and trajectory analysis. J. Mol. Model., 7: 306-317.
19. Jorgensen, W.L., D.S. Maxwell and J. Tirado-Rives, 1996. J. Am. Chem. Soc., 118(45): 11225-11236.
20 Kaminski, G.A., R.A. Friesner, J. Tirado-Rives and W.L. Jorgensen, 2001. J. Phys. Chem. B, 105(28): 6474-6487.
21. Berman, H., J. Westbrook, Z. Feng, G. Gililand, T. Bahat, H. Weissig and P. Shindyalov 2000. The protein data bank. Nucl. Acids Res., 28: 2235-242.
22. Laskowski, R.A., M.W. MacArthur, D.S. Moss and J.M. Thornton, 1993. PROCHECK: a program to check the stereo chemical quality of protein structures. J. Appl. Cryst., 26: 283-291.
23. Morris, G.M., D.S. Goodsell, R.S. Halliday, R. Huey, W.E. Hart, R.K. Belew and A.J. Olson, 1998. Automated docking using a Lamarckian genetic algorithm and an empirical binding free energy Fuction. J. Computer Chem., 19: 1639-1662
24. Bar-On, P., C.B. Millard, M. Harel, H. Dvir, A. Enz, J.L. Sussman and I. Silman, 2000. Kinetic and structural studies on the interaction of cholinesterases with the anti-Alzheimer drug rivastigmine. Biochemistry, 41(11): 3555-64.
25. Kryger, G., I. Silman and J.L. Sussman, 1999. Structure of acetylcholinesterase complexed with E2020 (Aricept): implications for the design of new anti-Alzheimer drugs. Structure, 7(3): 297-307.
26. Lipinski, C.A., F. Lombardo, B.W. Dominy and P.J. Feeney, 2001. Experimental and computational approaches to estimate solubility and permeability in drug discovery and development settings. Adv. Drug. Del. Rev., 46: 3-26.
27. Ekins, S., C.L. Waller, P.W. Swaan, G. Cruciani, S.A. Wrighton and J.H. Wikel, 2000. Progress in predicting human ADME parameters in silico. Journal of Pharmacological and Toxicological Methods, 44 (1): 251-272.

28. Thompson, J.D., D.G. Higgins and T.J. Gibson, 1994. CLUSTAL W: improving the sensitivity of progressive multiple sequence alignment through sequence weighting, position-specific gap penalties and weight matrix choice. Nucleic Acids Res., 22(22): 4673-4680.
29. Van Aalten, D.M., R. Bywater, J.B. Findlay, M. Hendlich, R.W. Hooft and G. Vriend, 1996. PRODRG, a program for generating molecular topologies and unique molecular descriptors from coordinates of small molecules. Journal of Computer-Aided Molecular Design, 10(3): 255-262.
30. Verdonk, M.L., J.C. Cole, M.J. Hartshorn, W.C. Murray and R.D. Taylor, 2003. Improved Protein-Ligand docking using GOLD. PROTEINS: Structure, Function and Genetics, 52: 609-62.
31. V. Life MDS: Molecular Design Suite, VLife Sciences Technologies Pvt. Ltd. Pune, India, 2010 (www.vlifesciences.com).
32. Wenk, G.L., 2003. Neuropathologic changes in Alzheimer's disease. J. Clin. Psychiatry, 64(9): 7-10.
33. Youdim, M. and J. Buccafsco, 2005. CNS Targets for multi-fuctional drugs in the treatment of Alzheimer's and Parkinson's diseases. J. Neural Transm, 112: 519-537.
34. Zheng, W. and A. Tropsha, 2000. Novel varaiable selection Quantitative Structure-Property Relationship Approach Based on the k-Nearest-Neighbor Principle. J. Chem. Inf. Comput. Sci., 40: 185-194.